

Current flow instability and nonlinear structures in dissipative two-fluid plasmas

O. Koshkarov, A. I. Smolyakov, I. V. Romadanov, O. Chapurin, M. V. Umansky, Y. Raitses, and I. D. Kaganovich

Citation: *Physics of Plasmas* **25**, 011604 (2018);

View online: <https://doi.org/10.1063/1.5017521>

View Table of Contents: <http://aip.scitation.org/toc/php/25/1>

Published by the [American Institute of Physics](#)

Articles you may be interested in

[Weak turbulence theory for beam-plasma interaction](#)

Physics of Plasmas **25**, 011603 (2017); 10.1063/1.5017518

[Dynamic stabilization of filamentation instability](#)

Physics of Plasmas **25**, 011601 (2017); 10.1063/1.5017517

[Electron holes in phase space: What they are and why they matter](#)

Physics of Plasmas **24**, 055601 (2017); 10.1063/1.4976854

[The asymptotic behavior of Buneman instability in dissipative plasma](#)

Physics of Plasmas **24**, 102102 (2017); 10.1063/1.5001950

[Rayleigh-Taylor instability and internal waves in strongly coupled quantum plasma](#)

Physics of Plasmas **24**, 112101 (2017); 10.1063/1.5000414

[Solitary structures in an inhomogeneous plasma with pseudo-potential approach](#)

Physics of Plasmas **24**, 114502 (2017); 10.1063/1.4993812

**COMPLETELY
REDESIGNED!**



**PHYSICS
TODAY**

Physics Today Buyer's Guide
Search with a purpose.

Current flow instability and nonlinear structures in dissipative two-fluid plasmas

O. Koshkarov,^{1,a)} A. I. Smolyakov,¹ I. V. Romadanov,¹ O. Chapurin,¹ M. V. Umansky,² Y. Raitses,³ and I. D. Kaganovich³

¹Department of Physics and Engineering Physics, University of Saskatchewan, Saskatoon, Saskatchewan S7N 5E2, Canada

²Lawrence Livermore National Laboratory, Livermore, California 94550, USA

³Plasma Physics Laboratory, Princeton University, Princeton, New Jersey 08543, USA

(Received 26 April 2017; accepted 13 July 2017; published online 13 December 2017)

The current flow in two-fluid plasma is inherently unstable if plasma components (e.g., electrons and ions) are in different collisionality regimes. A typical example is a partially magnetized $\mathbf{E} \times \mathbf{B}$ plasma discharge supported by the energy released from the dissipation of the current in the direction of the applied electric field (perpendicular to the magnetic field). Ions are not magnetized so they respond to the fluctuations of the electric field ballistically on the inertial time scale. In contrast, the electron current in the direction of the applied electric field is dissipatively supported either by classical collisions or anomalous processes. The instability occurs due to a positive feedback between the electron and ion current coupled by the quasi-neutrality condition. The theory of this instability is further developed taking into account the electron inertia, finite Larmor radius and nonlinear effects. It is shown that this instability results in highly nonlinear quasi-coherent structures resembling breathing mode oscillations in Hall thrusters. *Published by AIP Publishing.*

<https://doi.org/10.1063/1.5017521>

I. INTRODUCTION

Systems which are away from the equilibrium naturally evolve back toward the equilibrium state by compensating the deviation from the equilibrium. In plasmas which support many different wave eigen-modes, the deviations from the equilibrium often result in the development of various instabilities. The nature of such instabilities depends on the type of plasma state and its deviation from the equilibrium. One class of instabilities results from the non-equilibrium which can be characterized by gradients in the velocity space, e.g., plasma-beam instabilities or instabilities due to plasma pressure anisotropy.¹ The non-equilibrium states with relative streaming of electrons and ions are often unstable too. Buneman type instabilities² occur due to the relative motion of electrons and ions in collisionless plasma. In strongly collisional plasmas, the electron drift gives the Farley-Buneman instability.^{3,4} Simon-Hoh type instabilities (both the collisional^{5,6} and collisionless version⁷⁻⁹) result from the relative motion of electrons and ions in crossed electric and magnetic fields $\mathbf{E} \times \mathbf{B}$. The Simon-Hoh instability is typically studied for modes propagating in the direction of the $\mathbf{E} \times \mathbf{B}$ drift and typically requires a density gradient (and/or a magnetic field gradient^{8,9}) for the excitation.

Here, we discuss the axial instability of the modes along the direction of the current flow. Essentially, instabilities of this type were considered in Refs. 10 and 11. The basic instabilities in Refs. 10 and 11 exist in neglect of the electron inertia. The resistive instability of the lower-hybrid mode, which requires the electron inertia (but no density gradient) considered in Ref. 12, can also be referred to as the current

flow instability of this type. Such instabilities occur due to the phase shift in the response of electrons and ions to the quasi-neutral perturbation of the electric field. In this paper, we consider the axial flow instability in conditions typical of the $\mathbf{E} \times \mathbf{B}$ discharge, such as in Hall thrusters and magnetrons. In this case, the axial current is due to the dissipative flow of electrons and the flow of accelerated ions, both in the direction of the externally applied electric field. We consider the linear and nonlinear regimes of this instability and show that it results in nonlinear quasi-coherent structures. It was earlier suggested¹⁰ that this instability mechanism plays an important role in breathing mode oscillations.¹³

II. INSTABILITY MECHANISM

Most simply, the mechanism can be described on the example of the current flow in the $\mathbf{E} \times \mathbf{B}$ device such as a Hall thruster. Considering the configuration supported by the electric current in the axial direction (along z) due to the electric field $\mathbf{E} = E\hat{z}$ applied across the magnetic field. We generally characterize the electron current in the z direction in the form $J_e = \sigma E$, where σ can be simply collisional electron conductivity across the magnetic field, $\sigma_c = e^2 n_0 \nu_{en} / (m_e \omega_{ce}^2)$, or some anomalous conductivity which may include as well the effects of near wall conductivity.¹³ In the rest of the paper, we do not specify the mechanism of the electron transport, generally parameterizing it with σ (or ν introduced latter). The ion current $J_i = env_i$ is supported by free streaming of unmagnetized ions. We consider quasi-neutral oscillations so that

$$\frac{\partial}{\partial z} (J_e + env_i) = 0. \quad (1)$$

^{a)}Electronic mail: koshkarov.alexandr@usask.ca

The dynamics of unmagnetized ions is described by standard equations

$$\frac{\partial}{\partial t} n + \frac{\partial}{\partial z} (nv_i) = 0, \quad (2)$$

$$\frac{\partial}{\partial t} v_i + v_i \frac{\partial}{\partial z} v_i = \frac{e}{m_i} E. \quad (3)$$

Linearizing equations (1)–(3) for perturbations (denoted by tilde) in the form $(\tilde{n}, \tilde{E}, \tilde{v}_i, \tilde{J}_e) \sim \exp(-i\omega t + kz)$, and taking into account that ions have the equilibrium velocity v_{i0} , one easily finds the dispersion relation

$$\frac{1}{(\omega - kv_{i0})^2} = \frac{i}{\omega} \frac{\sigma m_i}{e^2 n_0}. \quad (4)$$

The right hand side of the dispersion equation can also be written as

$$\frac{\sigma m_i}{e^2 n_0} = \frac{\nu}{\omega_{LH}^2}, \quad (5)$$

where $\omega_{LH}^2 = \omega_{ce}\omega_{ci}$ and ν is either the frequency of the electron-neutral collisions, or parametrization of combined effects of anomalous collisions and near-wall conductivity. This dispersion relation was obtained in Ref. 10 by using the kinetic theory for ions and later in Ref. 11 from the fluid model.

The axial modes described by the dispersion relation (4) are unstable due to the phase shift between the perturbed

electron and ion currents, which can be seen from the following expressions:

$$\tilde{J}_e = \sigma \tilde{E}, \quad (6)$$

$$\tilde{J}_i = \frac{e^2 n_0}{m_i} \frac{i\omega}{(\omega - kv_{i0})^2} \tilde{E}. \quad (7)$$

The delay introduced by the finite ion flow results in the positive feedback loop leading to the amplification of the initial perturbation. In the absence of the flow $v_{i0} = 0$, the dispersion relation (4) describes a damped mode with

$$\omega = -i \frac{\omega_{LH}^2}{\nu}. \quad (8)$$

However, in the presence of a large equilibrium ion flow, $kv_{i0} > \omega$, one has the negative-diffusion-type instability. From Eq. (4), the growth rate scales with the wave vector as $\gamma \approx \nu k^2 v_{i0}^2 / \omega_{LH}^2$ for small $kv_{i0} \ll \omega_{LH}^2 / \nu$ and as $\gamma \approx \omega_{LH} \sqrt{kv_{i0} / (2\nu)}$ for large $kv_{i0} \gg \omega_{LH}^2 / \nu$. These asymptotics are valid for small $k\rho_e \ll 1$, but for larger values $k\rho_e \sim 1$, other effects become important as discussed in Sec. III. The solution to (4) is shown in Fig. 1(a).

III. MODE STABILIZATION AT SHORT WAVELENGTHS DUE TO THE EFFECTS OF DIFFUSION, INERTIA, AND FINITE LARMOR RADIUS

The instability with $\gamma \sim k^2$ (or $\sim \sqrt{k}$) in combination with nonlinear effects may produce explosive growth of the

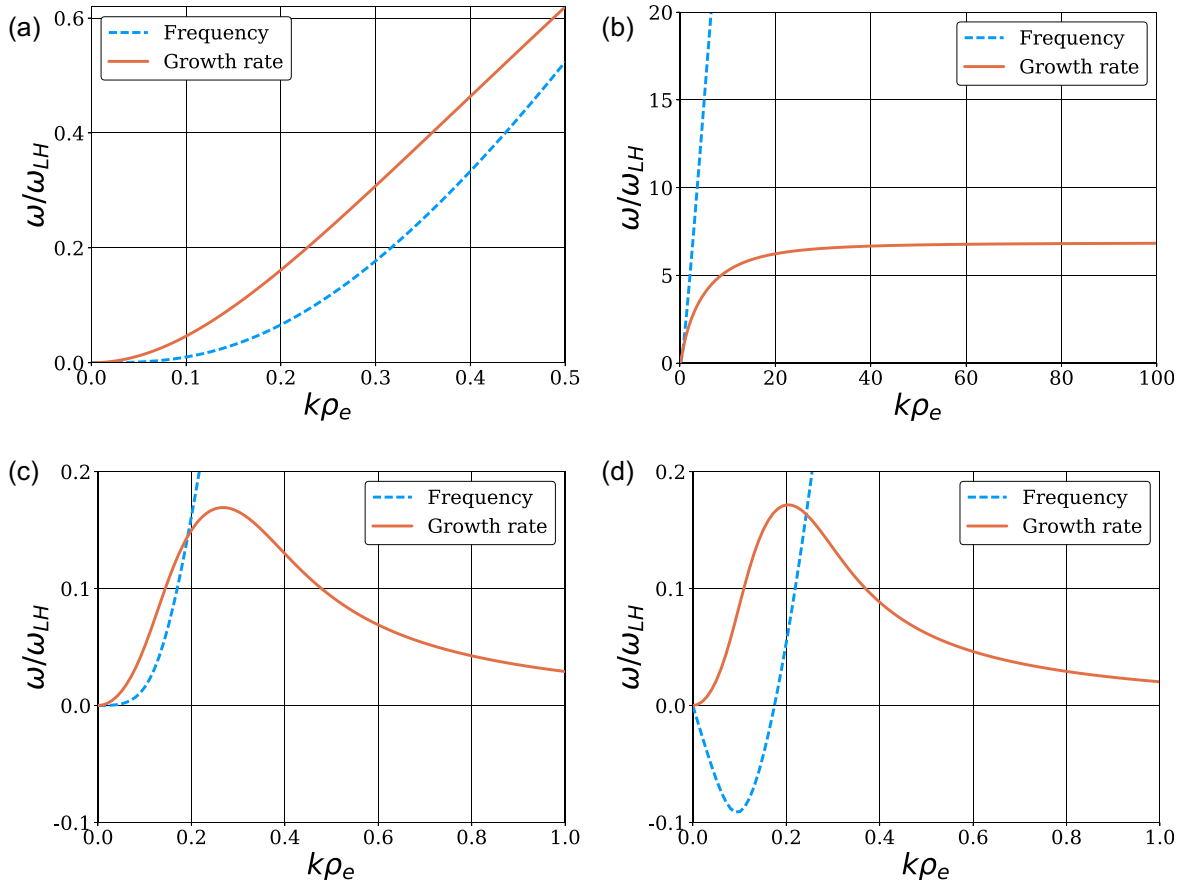


FIG. 1. Solutions to dispersion equations (4), (11), (13), and (14) for different electron transport models are shown for typical Hall thruster parameters: $v_{i0} = 4.45\omega_{LH}\rho_e$, $v_{e0} = -1.33\omega_{LH}\rho_e$, $\nu = 0.25\omega_{LH}$. (a) Simplest electron transport model $J_e = \sigma E$, $\gamma \sim k^2$ Eq. (4), (b) Eq. (11) with electron diffusion, (c) Eq. (13) with electron diffusion, inertia, and finite Larmor radius, and (d) Eq. (14) with electron diffusion, inertia, finite Larmor radius, and finite electron velocity.

perturbations. However, the unlimited growth rate (with k) is unphysical and it also presents a problem in numerical simulations because the instability will occur at the largest possible wave-vectors ($k_{max} \sim 1/\Delta x$, where Δx is the smallest resolution length scale, e.g., mesh size). This will result in piling up of the energy at the smallest resolution length scale. Therefore, the simulation results will never converge to a single solution. It is therefore important to incorporate physics which is relevant on smaller scales, thus limiting the growth at large wave-vectors. One of such effects is the diffusion flux which was first added in Ref. 11. The effects of the diffusion can be included via the pressure driven electron current in the generalized Ohm's law

$$J_e = \sigma E + eD \frac{\partial n}{\partial z}, \quad (9)$$

where

$$D = \nu \rho_e^2. \quad (10)$$

Once again, the ν should be understood either as the classical electron-neutral, near-wall or anomalous collisional frequency. Repeating the derivations in (1)–(3), one can get the following dispersion equation which takes into account both electron mobility and diffusion:

$$\frac{1}{(\omega - kv_{0i})^2} = \frac{i\nu}{\omega_{LH}^2 (\omega + i\nu k^2 \rho_e^2)}. \quad (11)$$

The solution of this equation is shown in Fig. 1(b). One can see from (11) that the diffusion does not stabilize high $k\rho_e$ completely, but limits the mode growth at the constant level

$$\gamma \approx \frac{\omega_{LH}(v_{0i} - \omega_{LH}\rho_e)}{2\nu\rho_e}. \quad (12)$$

Therefore, it is important to incorporate higher order effects such as electron inertia and related effects of the electron finite Larmor radius (FLR), which bring in the lower-hybrid modes.^{12,14} These effects may be included following the derivations in Ref. 9. The respective equation that includes the electron inertia, mobility, diffusion, and FLR reads

$$\frac{1}{(\omega - kv_{0i})^2} = \frac{(\omega + i\nu)}{\omega_{LH}^2 [\omega + k^2 \rho_e^2 (\omega + i\nu)]}. \quad (13)$$

The solution to Eq. (13) is shown in Fig. 1(c), which shows that electron inertia and FLR effects stabilize the modes for high $k\rho_e$. It is important to note that the electron inertia and FLR effects alone (without electron transport $\nu=0$) do not make the system unstable.

Our derivations so far have fully neglected the effect of the equilibrium electron velocity. It can be easily included in the consideration, resulting in the dispersion equation

$$\frac{1}{(\omega - kv_{0i})^2} = \frac{(\omega - kv_{0e} + i\nu)}{\omega_{LH}^2 [\omega - kv_{0e} + k^2 \rho_e^2 (\omega - kv_{0e} + i\nu)]}. \quad (14)$$

The results for the final dispersion equation (14) are shown in Fig. 1(d). Note that in the absence of dissipation, this equation describes stable lower-hybrid modes modified by

the Doppler shift and the effects of the finite electron Larmor radius.⁹ The addition of the electron equilibrium velocity results in the Doppler shift kv_{0e} in the electron response which has a significant impact on the real part of the frequency of unstable modes: for v_{0e} has the opposite sign to v_{0i} , the account of the equilibrium electron flow reduces the phase velocity of unstable modes and may even result in the change of the sign of the phase velocity.

The final dispersion equation (14) depends on three important parameters: ion equilibrium velocity v_{0i} , electron equilibrium velocity v_{0e} , and electron collision frequency ν (classical or anomalous). Therefore, to complete the physical picture of effects discussed in this section, we demonstrate how external parameters change the frequency and growth rate of the unstable mode. The effect of collisional frequency is shown in Figs. 2(a) and 2(b), where we varied the parameter from the typical Hall thruster classical value $\nu \approx 0.1\omega_{LH}$ up to the anomalous $\nu = 2.5\omega_{LH}$. One can see that the increase of the collision frequency enhances the linear instability and moves the most unstable wave number to the shorter wavelengths. At larger values, the collisions suppress the instability, as shown in Figs. 2(c) and 2(d). It is worth noting that the results for high (anomalous) collisionality $\nu \gg \omega_{LH}$, should be viewed as the illustration of a general trend rather than a quantitative description of the nonlinear effects (anomalous mobility). Though the often used Bohm diffusion would correspond to anomalously high values of the electron collision frequency (as large as ω_{ce}), the form of the nonlinear (anomalous) mobility and its proper parametrization is still unknown at this time. Next, we investigate the effects of the ion equilibrium velocity, which is shown in Fig. 3. To see the effect more clearly, the electron equilibrium velocity was set to zero. The ion flow velocity enhances the instability moving the maximum growth rate to the longer wavelengths, where the effects of a finite length of the system may become important.^{15,16} We will employ the correct boundary conditions in Sec. IV. The experimental data indicates¹⁷ that typically the electron flow is a fraction of the ion flow ($v_{0e} \approx -(0.3 - 0.5)v_{0i}$). The larger values of the equilibrium electron flow shift the maximum of the growth rate toward the longer wavelengths and also reverse the phase velocity to the negative direction for the most unstable modes, as is shown in Fig. 4.

IV. NONLINEAR EVOLUTION AND STRUCTURES

The linear theory described in Sec. III predicts axial flow instability with a maximal growth rate which is determined by the competition of the instability and stabilizing effects of the diffusion, inertia, and FLR effects. To investigate the nonlinear evolution of these modes, we perform nonlinear simulations using the model which was developed in Ref. 9 and includes the nonlinear equations for ion density (continuity) and velocity in addition to the electron dynamics equation. In the one dimensional case, the nonlinear ion continuity and momentum balance equations (2) and (3) have the form

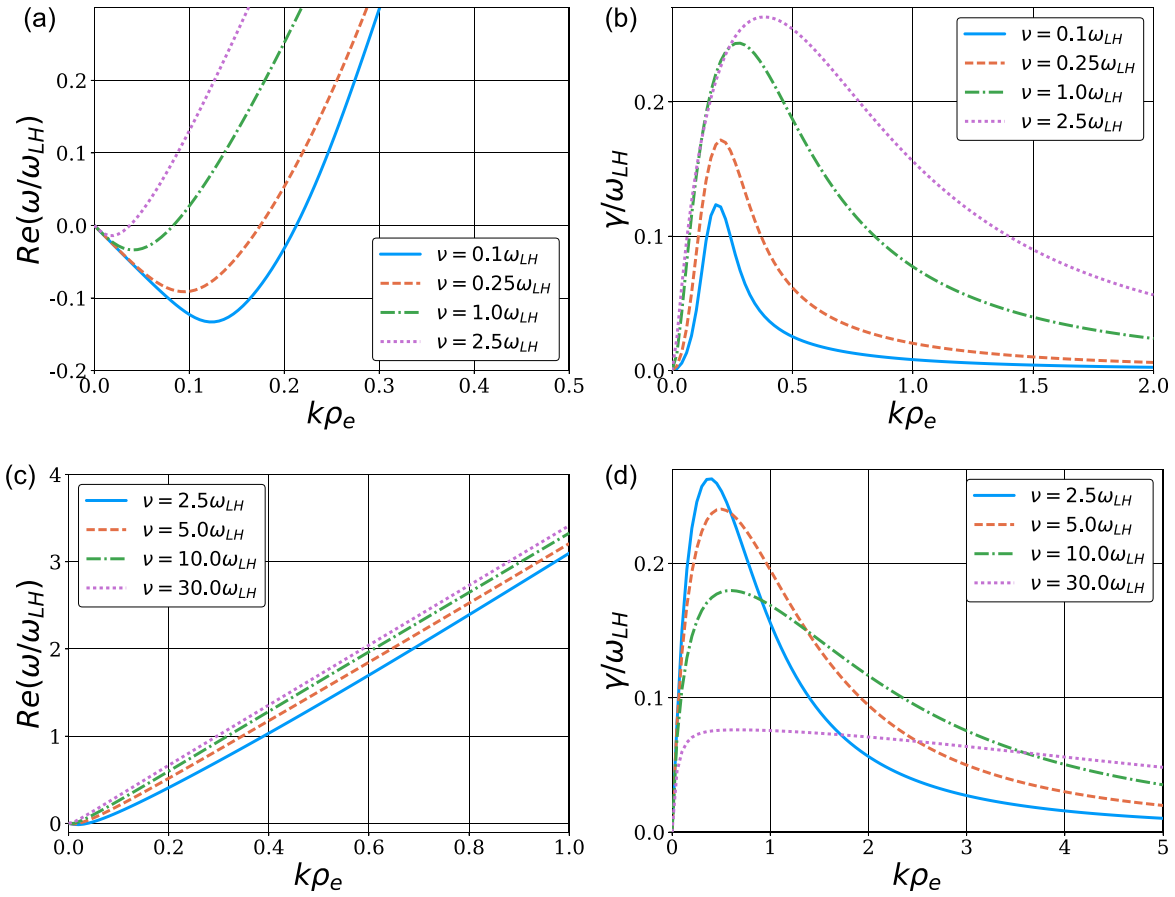


FIG. 2. Solution to the dispersion equations (14) for different values of electron collision frequency ν and typical Hall thruster parameters: $v_{i0} = 4.45\omega_{LH}\rho_e$ and $v_{e0} = -1.33\omega_{LH}\rho_e$. (a) Frequency, (b) growth rate, (c) frequency, and (d) growth rate.

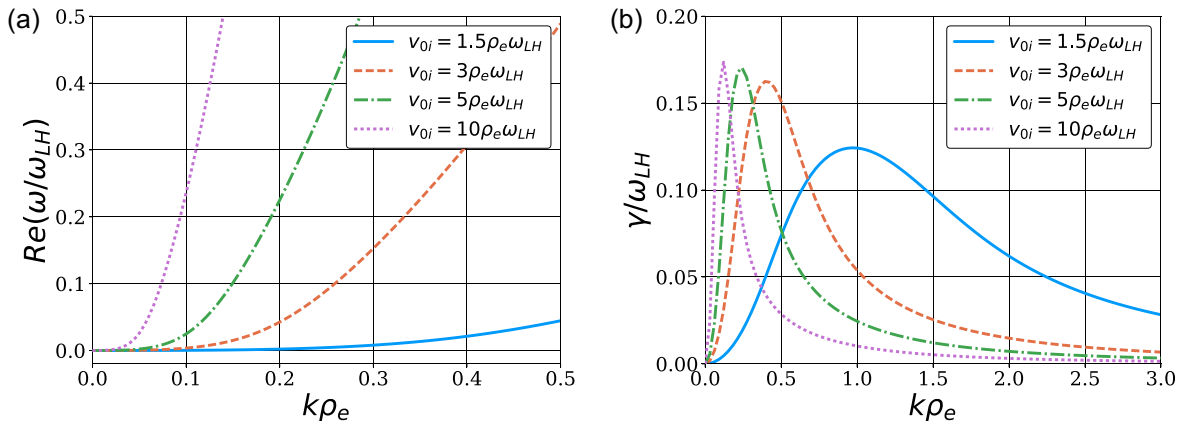


FIG. 3. Solution to the dispersion equation (14) for different values of equilibrium ion velocity, zero equilibrium electron velocity, and collision frequency $\nu = 0.25\omega_{LH}$. (a) Frequency and (b) growth rate.

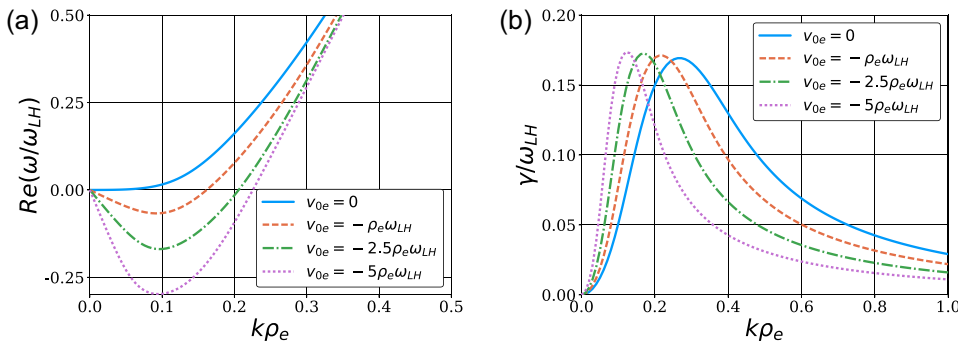


FIG. 4. Solution to the dispersion equation (14) for different values of equilibrium electron velocity and typical Hall thruster parameters $v_{i0} = 4.45\omega_{LH}\rho_e$, $\nu = 0.25\omega_{LH}$. (a) Frequency and (b) growth rate.

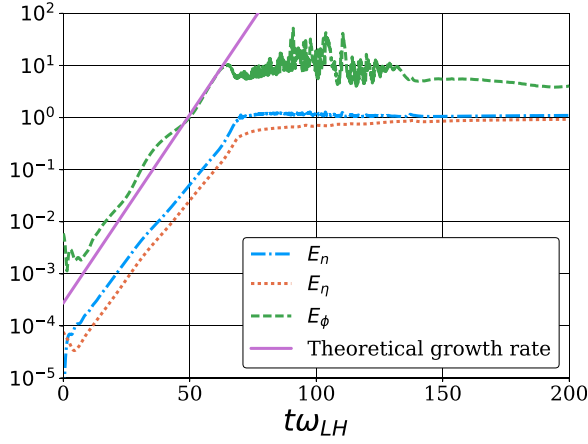


FIG. 5. The dashed lines represent time evolution of energy like functionals (20) for parameters: $\nu = 0.25\omega_{LH}$, $v_{0i} = 4.45\omega_{LH}\rho_e$, $v_{0e} = -0.3v_{0i}$, $L = 106\rho_e$; the purple solid line is the maximum theoretical growth rate obtained from Eq. (14).

$$\left(\frac{\partial}{\partial t} + v_{0i}\frac{\partial}{\partial z}\right)\tilde{n} = n_0\frac{\partial^2\tilde{\chi}}{\partial z^2} + \tilde{n}\frac{\partial^2\tilde{\chi}}{\partial z^2} + \frac{\partial\tilde{n}}{\partial z}\frac{\partial\tilde{\chi}}{\partial z}, \quad (15)$$

$$\left(\frac{\partial}{\partial t} + v_{0i}\frac{\partial}{\partial z}\right)\tilde{\chi} = \frac{e}{m_i}\tilde{\phi} + \frac{1}{2}\left(\frac{\partial\tilde{\chi}}{\partial z}\right)^2, \quad (16)$$

where the potential was introduced for the ion velocity $\tilde{v}_i = -\partial\tilde{\chi}/\partial z$. The electron transport model includes the electron diffusion, inertia, and FLR effects. In the Boussinesq approximation, the electron dynamics is linear and described by the equation

$$\left(\frac{\partial}{\partial t} + v_{0e}\frac{\partial}{\partial z}\right)\tilde{\eta} = -\nu(\tilde{\eta} - \tilde{n}) \quad (17)$$

with the electron generalized vorticity defined as

$$\tilde{\eta} = \tilde{n} + n_0\rho_e^2\frac{\partial^2}{\partial z^2}\left(\frac{e\tilde{\phi}}{T_e} - \frac{\tilde{n}}{n_0}\right). \quad (18)$$

The typical Hall thruster axial length is around $L \sim (25-100)\rho_e$; therefore, for modes with the wave number $k\rho_e \approx 0.1$, the realistic boundary conditions are important. We use boundary conditions corresponding to the absence of

perturbation at the left ($z=0$) and open boundary at the right ($z=L$)

$$\begin{aligned} \tilde{n}(0) = \tilde{n}'(L) = \tilde{\chi}(0) = \tilde{\chi}'(L) = \tilde{\eta}(0) = \tilde{\eta}'(L) = \tilde{\phi}(0) \\ = \tilde{\phi}'(L) = 0, \end{aligned} \quad (19)$$

where prime denotes the spatial derivatives.

We performed the nonlinear simulations of the system (15)–(19) using the BOUT++ plasma fluid simulation framework,¹⁸ which was modified for the case of partially magnetized plasma⁹ and extensively benchmarked. The nonlinear simulations are monitored with energy like functionals

$$E_n = E\left[\frac{\tilde{n}}{n_0}\right], \quad E_\eta = E\left[\frac{\tilde{\eta}}{n_0}\right], \quad E_\phi = E\left[\frac{e\tilde{\phi}}{T_e}\right], \quad (20)$$

with

$$E[f] = \sqrt{\frac{1}{L}\int_0^L dz|f(z)|^2}. \quad (21)$$

The time evolution of (20) is shown in Fig. 5 for typical Hall thruster parameters: $\nu = 0.25\omega_{LH}$, $v_{0i} = 4.45\omega_{LH}\rho_e$, $v_{0e} = -0.3v_{0i}$, and $L = 106\rho_e$. One can see a distinct linear growth phase in the initial stage $t\omega_{LH} \sim 0-70$. The maximum theoretical growth rate obtained from Eq. (14) is shown in the Fig. 5 by a purple solid line, which shows a good agreement between the theory and simulations. At later times $t\omega_{LH} \geq 70$, when $E_n \sim E_\eta \sim 1$, nonlinear dynamics start to dominate and fluctuations saturate at constant values. The evolution of density \tilde{n} and generalized electron vorticity $\tilde{\eta}$ in time and space is shown in Figs. 6 and 7. As shown in Fig. 6, in the linear stage ($\tilde{n}/n_0 \sim \tilde{\eta}/n_0 \ll 1$), density and vorticity perturbations are growing and slowly moving to the right. This corresponds to the linear picture shown in Fig. 1(d), where the most unstable modes have a small positive phase velocity. As amplitude fluctuations increase ($\tilde{n}/n_0 \sim \tilde{\eta}/n_0 \sim 1$), the nonlinear effects become important resulting in the formation of strongly nonlinear quasi-periodic waves, see Fig. 7. It is interesting to note that as the mode amplitude grows and nonlinear effects become more important, the velocity of nonlinear waves reduces and eventually

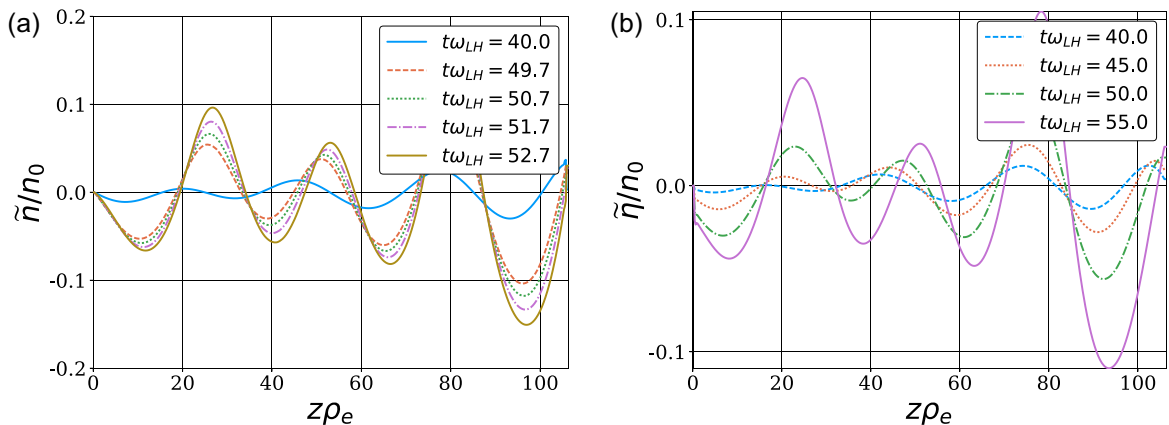


FIG. 6. Linear dynamics of density \tilde{n} and generalized vorticity $\tilde{\eta}$ spatial profiles. (a) Density and (b) vorticity.

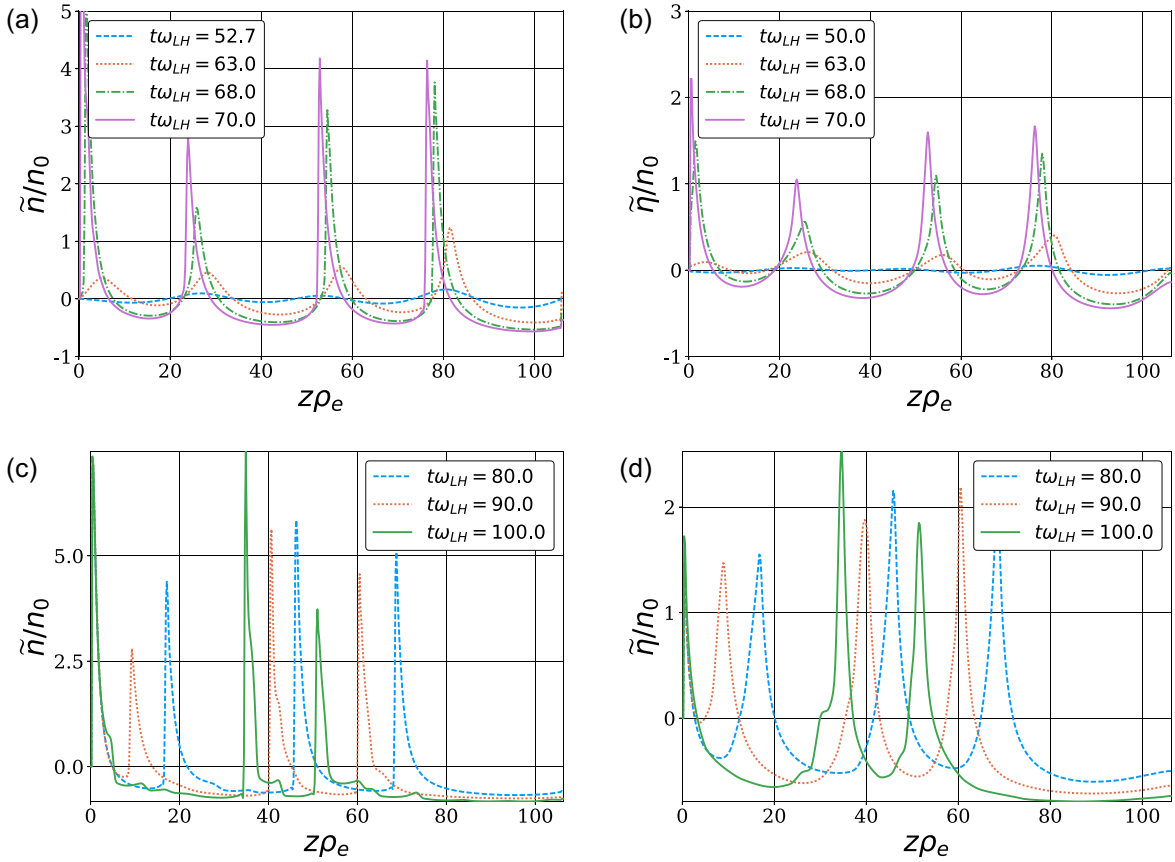


FIG. 7. Nonlinear dynamics of density \tilde{n} and generalized vorticity $\tilde{\eta}$ spatial profiles. (a) Density, (b) vorticity, (c) density, and (d) vorticity.

becomes negative, so they start moving in the opposite direction (to the left). This effect is attributed to the electron equilibrium flow, which is in the negative direction (to the left).

The nonlinear evolution in the case of zero electron flow $v_{0e} = 0$ is similar, with the exception that the velocity of nonlinear structures does not change the direction.

V. CONCLUSION

We have analyzed the axial instability of the current flow due to the phase shift in the electron and ion response to the perturbations of the electric field. This is a particular example of a general class of instabilities for the modes propagating along the direction of the current flow, which do not need a density gradient as is required for Simon-Hoh instabilities.^{5,6} The dispersion relation similar to (4), was obtained in Ref. 10, where it was concluded that this instability is an important ingredient of breathing oscillations.¹⁹ A similar dispersion equation was also obtained in Ref. 11, where the effects of the diffusion was added. As was noted in Ref. 10, the dispersion relation (4) is analogous to the one obtained in Ref. 12 for the resistive instability of the azimuthal modes driven by the $\mathbf{E} \times \mathbf{B}$ flow.

Our model for the instability additionally includes the effects of the electron inertia and finite Larmor radius which are important for the correct description of the modes at high k values.

It is important to note that the discussed instability occurs due to the phase shift between the inertial response of

ions and dissipative electron response. The exact mechanism of electron current (classical collisional) or anomalous (turbulent)²⁰ is not so critical as long as the perturbations of the electron current are in phase with the electric field. Thus, one can expect that this mechanism will be operative when the electron flow is anomalous and some scale/time separation exists between fast electron processes that determine anomalous transport and slow the evolution of this instability.

The axial flow instability discussed in this paper has a relatively low growth rate compared to azimuthal modes of higher frequencies which are driven by collisions and density gradients.^{8,9} Its significance, however, is in the high amplitude of the saturated modes. The mode saturation occurs due to ion dynamics resulting in the appearance of high amplitude quasi-coherent structures resembling the cnoidal waves.²¹ The theory of such highly nonlinear (non-perturbative) waves is described in Ref. 21. The nonlinear coherent structures observed in our simulations appear to be an example of such large amplitude waves born out of the instability. The electron nonlinearity is weak as it appears in the higher order polarization drift and only for the non-Boussinesq approximation. In this paper, we consider the Boussinesq approximation so the electron dynamics is linear while, all explicit nonlinear effects originate in ion dynamics. The electron inertia and FLR effects are important here as a mechanism of stabilization of the instability at large k (due to coupling to lower-hybrid dynamics).

It has been suggested¹⁰ that the instability of this type is a crucial ingredient of breathing oscillations often observed

in Hall thruster discharges supported by the axial electron current. Our basic model given by Eqs. (1)–(3) is a subset of the full systems of equations typically considered for the description of the breathing mode.^{13,17,22} Our simulations show that the considered instability results in the formation of nonlinear quasi-coherent structures which are indeed similar to those observed in the breathing mode.^{19,23} The slow moving coherent structures formed as a result of axial flow instability discussed here could also be the sources of non-monotonous profiles of the electric field observed experimentally in Ref. 24.

The finite velocity of ions plays a critical role in the axial current flow instability discussed in our paper. The characteristic time scale associated with ion velocity, $\omega \simeq v_i/L$, where L is the characteristic length, is typically considered to be in the range of the so called transit instabilities,^{25,26} which have higher frequencies compared to the breathing oscillations. In our model, the real part of the unstable modes is considerably lower than $\omega \simeq v_i/L$, in part due to inclusion of the electron flow velocity. One should note though that in the present paper, we consider the case of constant ion velocity v_{0i} , while in real configurations, the effects of the axial dependence $v_{i0}(x)$ could be important.^{25,26} In consideration of this, a more general case, is left for future publication.

ACKNOWLEDGMENTS

This work was supported in part by the NSERC Canada and the U.S. Air Force Office of Scientific Research FA9550-15-1-0226.

¹A. B. Mikhailovskii, *Theory of Plasma Instabilities*, Vol. 1, Instabilities of a Homogeneous Plasma (Springer, New York, 1974).

²O. Buneman, "Instability, turbulence, and conductivity in current-carrying plasma," *Phys. Rev. Lett.* **1**(1), 8 (1958).

³O. Buneman, "Excitation of field aligned sound waves by electron streams," *Phys. Rev. Lett.* **10**(7), 285 (1963).

⁴D. T. Farley, "A plasma instability resulting in field-aligned irregularities in ionosphere," *J. Geophys. Res.* **68**(22), 6083, <https://doi.org/10.1029/JZ068i022p06083> (1963).

⁵A. Simon, "Instability of a partially ionized plasma in crossed electric and magnetic fields," *Phys. Fluids* **6**(3), 382 (1963).

⁶F. C. Hoh, "Instability of penning-type discharges," *Phys. Fluids* **6**(8), 1184 (1963).

⁷Y. Sakawa, C. Joshi, P. K. Kaw, F. F. Chen, and V. K. Jain, "Excitation of the modified Simon-Hoh instability in an electron-beam produced plasma," *Phys. Fluids B-Plasma Phys.* **5**(6), 1681 (1993).

⁸W. Frias, A. I. Smolyakov, I. D. Kaganovich, and Y. Raitsev, "Long wavelength gradient drift instability in Hall plasma devices. I. Fluid theory," *Phys. Plasmas* **19**(7), 072112 (2012).

⁹A. I. Smolyakov, O. Chapurin, W. Frias, O. Koshkarov, I. Romadanov, T. Tang, M. Umansky, Y. Raitsev, I. D. Kaganovich, and V. P. Lakhin, "Fluid theory and simulations of instabilities, turbulent transport and coherent structures in partially-magnetized plasmas of $E \times B$ discharges," *Plasma Phys. Controlled Fusion* **59**(1), 014041 (2017).

¹⁰S. Chable and F. Rogier, "Numerical investigation and modeling of stationary plasma thruster low frequency oscillations," *Phys. Plasmas* **12**(3), 033504 (2005).

¹¹E. Fernandez, M. K. Scharfe, C. A. Thomas, N. Gascon, and M. A. Cappelli, "Growth of resistive instabilities in $E \times B$ plasma discharge simulations," *Phys. Plasmas* **15**(1), 012102 (2008).

¹²A. A. Litvak and N. J. Fisch, "Resistive instabilities in Hall current plasma discharge," *Phys. Plasmas* **8**(2), 648 (2001).

¹³A. I. Morozov and V. V. Savel'yev, "Reviews of plasma physics," in *Reviews of Plasma Physics*, edited by B. B. Kadomtsev and V. D. Shafranov (Kluwer, New York, 2000), Vol. 21, p. 203.

¹⁴R. C. Davidson and N. T. Gladd, "Anomalous transport properties associated with lower-hybrid-drift instability," *Phys. Fluids* **18**(10), 1327–1335 (1975).

¹⁵A. Kapulkin and E. Behar, "Ion beam instability in Hall thrusters," *IEEE Trans. Plasma Sci.* **43**(1), 64 (2015).

¹⁶O. Koshkarov, A. I. Smolyakov, I. D. Kaganovich, and V. I. Ilgisonis, "Ion sound instability driven by the ion flows," *Phys. Plasmas* **22**(5), 052113 (2015).

¹⁷A. I. Morozov and V. V. Savel'yev, "One-dimensional hydrodynamic model of the atom and ion dynamics in a stationary plasma thruster," *Plasma Phys. Rep.* **26**(3), 219 (2000).

¹⁸B. D. Dudson, M. V. Umansky, X. Q. Xu, P. B. Snyder, and H. R. Wilson, "BOU++: A framework for parallel plasma fluid simulations," *Comput. Phys. Commun.* **180**(9), 1467 (2009).

¹⁹J. P. Boeuf and L. Garrigues, "Low frequency oscillations in a stationary plasma thruster," *J. Appl. Phys.* **84**(7), 3541 (1998).

²⁰G. J. M. Hagelaar, J. Bareilles, L. Garrigues, and J. P. Boeuf, "Modelling of stationary plasma thrusters," *Contrib. Plasma Phys.* **44**(5–6), 529 (2004).

²¹R. C. Davidson, *Methods in Nonlinear Plasma Theory* (Academic Press, New York, 2012).

²²A. I. Morozov and V. V. Savel'yev, "Numerical simulation of plasma flow dynamics, in SPT," IEPC'95 - International Electric Propulsion Conference, 24th (Moscow, Russia, 1996).

²³S. Barral and E. Ahedo, "Low-frequency model of breathing oscillations in Hall discharges," *Phys. Rev. E* **79**(4), 046401 (2009).

²⁴J. Vaudolon, B. Khier, and S. Mazouffre, "Time evolution of the electric field in a Hall thruster," *Plasma Sources Sci. Technol.* **23**(2), 022002 (2014).

²⁵S. Barral, K. Makowski, Z. Peradzynski, and M. Dudeck, "Transit-time instability in Hall thrusters," *Phys. Plasmas* **12**(7), 073504 (2005).

²⁶J. Vaudolon and S. Mazouffre, "Observation of high-frequency ion instabilities in a cross-field plasma," *Plasma Sources Sci. Technol.* **24**(3), 032003 (2015).